ORIGINAL ARTICLES

A RIGID BODY MODEL OF THE DYNAMIC POSTEROANTERIOR MOTION RESPONSE OF THE HUMAN LUMBAR SPINE

Tony S. Keller, PhD,[a] and Christopher J. Colloca, DC,[b]

ABSTRACT

Background: Clinicians apply posteroanterior (PA) forces to the spine for both mobility assessment and certain spinal mobilization and manipulation treatments. Commonly applied forces include low-frequency sinusoidal oscillations (<2 Hz) as used in mobilization, single haversine thrusts (<0.5 seconds) as imparted in high-velocity, low-amplitude (HVLA) manipulation, or very rapid impulsive thrusts (<5 ms) such as those delivered in mechanical-force, manually-assisted (MFMA) manipulation. Little is known about the mechanics of these procedures. Reliable methods are sought to obtain an adequate understanding of the force-induced displacement response of the lumbar spine to PA forces.

Objective: The objective of this study was to investigate the kinematic response of the lumbar spine to static and dynamic PA forces.

Design: A 2-dimensional modal analysis was performed to predict the dynamic motion response of the lumbar spine.

Methods: A 5-degree-of-freedom, lumped equivalent model was developed to predict the PA motion of the lumbar spine. Lumbar vertebrae were modeled as masses, massless-spring, and dampers, and the resulting equations of motion were solved by using a modal analysis approach. The sensitivity of the model to variations in the spring stiffness and damping coefficients was examined, and the model validity was determined by comparing the results to oscillatory and impulsive force measurements of vertebral motion associated with spine mobilization and 2 forms of spinal manipulation.

Results: Model predictions, based on a damping ratio of 0.15 (moderate damping) and PA spring stiffness coefficient ranging from 25 to 60 kN/m, showed good agreement with in vivo human studies. Quasi-static and low-frequency (<2.0 Hz) forces at L3 produced L3 segmental and L3-L4 intersegmental displacements up to 8.1 mm and 3.0 mm, respectively. PA oscillatory motions were over 2.5-fold greater for oscillatory forces applied at the natural frequency. Impulsive forces produced much lower segmental displacements in comparison to static and oscillatory forces. Differences in intersegmental displacements resulting from impulsive, static, and oscillatory forces were much less remarkable. The latter suggests that intersegmental motions produced by spinal manipulation may play a prominent role in eliciting therapeutic responses.

[a]Professor and Interim Chair, Department of Mechanical Engineering, University of Vermont, Burlington, Vt.

[b]Postgraduate and Continuing Education Department Faculty, New York Chiropractic College, Seneca Falls, NY, and private practice of chiropractic, Phoenix, Ariz.

This study was presented at the 12th Conference of the European Society of Biomechanics, Dublin, Ireland, August 27-30, 2000.

This research is supported in part by the National Institute of Chiropractic Research, NASA Experimental Program to Stimulate Competitive Research, and the Foundation for the Advancement of Chiropractic Education.

Submit reprint requests to: Tony S. Keller, PhD, Interim Chair, University of Vermont, Department of Mechanical Engineering, Burlington, VT 05405-0156.

Paper submitted June 25, 2001; in revised form October 1, 2001.

Copyright © 2002 by JMPT.

0161-4754/2002/$35.00 + 0 **76/1/127079**
doi:10.1067/mmt.2002.127079

Conclusions: The simple analytical model presented in this study can be used to predict the static, cyclic, and impulsive force PA displacement response of the lumbar spine. The model provides data on lumbar segmental and intersegmental motion patterns that are otherwise difficult to obtain experimentally. Modeling of the PA motion response of the lumbar spine to PA forces assists in the understanding the biomechanics of therapeutic PA forces applied to the lumbar spine and may ultimately be used to validate chiropractic technique procedures and minimize risk to patients receiving spinal manipulative therapy. (J Manipulative Physiol Ther 2002;25:485-96)

Key Indexing Terms: *Biomechanics; Dynamic Simulation; Manipulation; Modeling; Spine*

Introduction

Spinal manipulative therapy is a commonly used conservative treatment in patients with pain of musculoskeletal origin. Numerous spinal manipulative therapy techniques exist that produce different forces, loading vectors, and loading rates, providing clinicians with technique-specific choices for treatment of particular patient conditions and/or spinal level. Such techniques have been classified in national and international guidelines.[1,2] Posteroanterior (PA) forces are routinely applied to the spine during the course of spinal manipulative therapy, but very little is known about the dynamics of such procedures. During spinal manipulation or mobilization, the application of forces to the spine can be performed by using low-frequency or quasi-static sinusoidal oscillations (<2 Hz) such as those delivered in mobilization assessments or treatments,[3] single haversine thrusts (<0.5 seconds) such as those delivered with high-velocity, low-amplitude (HVLA) spinal manipulation,[4] or very rapid impulsive thrusts (<5 milliseconds [ms]) such as those delivered by means of a hand-held spinal adjusting instrument and categorized as mechanical-force, manually-assisted (MFMA) procedures.[5,6] However, little is known about the mechanics of these procedures.[4] Thus, reliable methods to obtain an adequate understanding of the force-induced displacement response of the spine have long been considered important.

A biomechanical analysis of the spine is important for understanding and predicting its response to different loading environments. Although substantial information exists on the dynamic response of the spine in the axial direction,[7] little is known about the dynamic response to externally applied PA forces such as those applied in the application of spinal mobilization or manipulation. In addition to treatment application, clinicians commonly apply quasi-static oscillatory PA forces to the spine to assess its mobility or stiffness, or to note the effect of applied force on the patient's symptoms. Without resorting to invasive techniques, precise assessment of clinically relevant variables, such as vertebral and intervertebral movements, is difficult to obtain.[8] Thus, development of a model is an important foundation for developing an understanding of the theoretical basis for mobilization and manipulation, as well as determining the stiffness of the spine.

A biomechanical model can be used to study the mechanical response of the spine under a variety of different loading environments, including static, oscillatory, and impact loading. Lee and Evans[9] developed a mathematical model of the lumbar spine's response to PA forces but did not validate it by comparison with human experiments. Lee et al[8] developed a 3-dimensional finite element model of the spine, ribcage, and pelvis, which was used to predict static segmental displacement responses of the lumbar vertebrae to PA forces. They validated their model by comparing predictions to low-frequency (<2 Hz) PA oscillatory force-displacement data observed in human subjects in vivo, finding good agreement with the mean observed human responses. Solinger[10] recently developed an analytical model describing the dynamics of small impulses applied to vertebrae and used experimental data to identify system parameters. The model was restricted to analysis of L2-L3 and did not consider coupling between adjacent vertebrae. A better understanding of the dynamic motion response of the spine is important to more thoroughly understand the nature of therapeutic effects associated with spinal manipulation and mobilization. The objective of this study was to model the dynamic vertebral and intervertebral motion response of the lumbar spine subjected to various spinal manipulative and mobilization forces. Model results are compared to quasi-static, oscillatory, and impulsive force measurements of vertebral motion.

Methods

Five Degree-of-Freedom Model

A 5-degree-of-freedom (DOF) mass, massless-spring, and damper model of the lumbar spine is shown in Figure 1. The 5 lumbar vertebral bodies are modeled as rigid structures connected by 6 flexible joint structures consisting of the intervertebral disks and other soft connective tissues that comprise the anterior and posterior columns of the functional spinal unit. The thorax and sacrum are assumed to be immobile. Each of the flexible joint structures (FJSs) are modeled using a massless-spring and damper (symbolically designated by a dashpot). The spring element of each FJS is assumed to have a linear force-deflection relationship, following Hooke's law, $F = kx$, where k is the stiffness coefficient (N/m) and x is the deflection (m). The damper

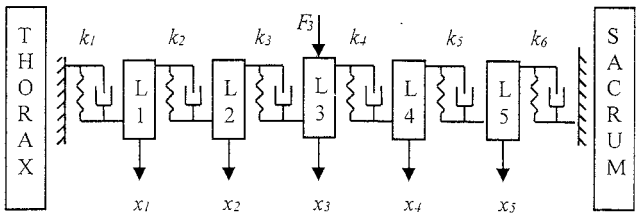

Fig 1. *Five-DOF, lumped mass, massless spring, and damper model of the spine.*

element is assumed to behave according to a linear force-velocity relationship (Newtonian viscous fluid), $F = c\mathrm{d}x/\mathrm{dt}$, where c is the viscous damping coefficient (Ns/m). From the solution of the equations of motion of this simple model, the static displacement response x and/or dynamic displacement response x (t) of each of the 5 lumbar segments can be determined for a given applied vertical or PA force F. PA forces can be applied to one or more of the spinous processes of vertebrae, but only PA forces applied to individual vertebrae are considered in this article.

Modeling of this multi-DOF structure necessitates 1 governing equation of motion to represent the inertial forces, dissipative forces, restoring forces, and external forces for each DOF. The matrix representation of the differential equations of vibration of a structure with more than one DOF is:

$$[M]\{\mathrm{d}^2x/\mathrm{d}t^2\} + [C]\{\mathrm{d}x/\mathrm{d}t\} + [K]\{x\} = \{F\} \qquad (1)$$

where $[M]$ is the mass matrix, $[C]$ is the viscous damping matrix, $[K]$ is the stiffness matrix, $\{F\}$ is the PA excitation force vector (column matrix), and $\{x\}$ is the resulting displacement vector. There are six stiffness coefficients k_i, i = 1. . .6, corresponding to each of the 6 FJSs.

The differential equations of motion for the 5-DOF system are in general coupled, such that each coordinate appears in each equation. Cross products of coordinates denote coupling, so the choice of coordinates establishes the type of coupling. Here we assume that the system has *zero mass coupling*, in which case $[M]$ is diagonal:

$$[M] = \begin{bmatrix} m_1 & 0 & 0 & 0 & 0 \\ 0 & m_2 & 0 & 0 & 0 \\ 0 & 0 & m_3 & 0 & 0 \\ 0 & 0 & 0 & m_4 & 0 \\ 0 & 0 & 0 & 0 & m_5 \end{bmatrix}$$

$[K]$ is written in terms of the stiffness influence coefficients, which are obtained from free body analysis of the structure in Figure 1, and is a band matrix along the diagonal:

$$[K] = \begin{bmatrix} (k_1 + k_2) & -k_2 & 0 & 0 & 0 \\ -k_2 & (k_2 + k_3) & -k_3 & 0 & 0 \\ 0 & -k_3 & (k_3 + k_4) & -k_4 & 0 \\ 0 & 0 & -k_4 & (k_4 + k_5) & -k_5 \\ 0 & 0 & 0 & -k_5 & (k_5 + k_6) \end{bmatrix}$$

For free vibration with no viscous damping $[C] = \{0\}$, a steady-state displacement solution for Equation 1 can be assumed to be a harmonic function, namely the product of a constant ψ_i and a function of time: $x_i = \psi_i \sin\omega t$, where ψ_i is the amplitude of oscillation of segment i, and ω is the circular frequency of oscillation. The fact that the governing equations for x_1(t). . .x_5(t) are the same mathematically, implies a *synchronicity of motion*. We therefore expect the displacement coordinates (x_i) to vary in a constant proportion as a function of time. Substitution of the previous system of equations into the equation of motion (Equation 1, $[C] = 0$) yields the characteristic value or eigenvalue problem:

$$[K - \Omega_i^2 M]\Psi_i = \{0\} \qquad (2)$$

where Ω_i is the natural frequency of vibration (eigenvalues) corresponding to mode shape ψ_i (eigenvectors), and i = 1. . .5. Hence, there are as many natural frequencies as DOFs; in our case, 5. To evaluate the allowable frequencies Ω_i that the system can support, we need to solve Equation 2. From the theory of matrices, we know that a nontrivial set of solutions exist if the determinant of the coefficients vanishes:

$$\left| [\mathrm{K}] - \Omega_i^2 [M] \right| = \{0\}.$$

This is known as the characteristic determinant, and the expansion is the characteristic equation. The solution of the characteristic equation results in the characteristic values Ω_i or eigenvalues, and these can be used to determine the characteristic vectors or eigenvectors ψ_i. Ω_i and ψ_i are readily obtained from Equation 2 as the diagonal matrix of eigenvalues (Ω_i^2) and the eigenvectors, respectively.

Since the equations of motion of each mass are identical, the ratio of the amplitudes ψ_i of each mass will be independent of time. The ratios between displacement amplitudes of various masses are called the *normal modes of vibration*. There is one ratio for each natural frequency, and we will use the notation ψ_{ij}/ψ_{kj} where the first subscript denotes the mass number and the second subscript denotes the frequency number. In this study, the modes of vibration are normalized with respect to mass m_5 ($k = 5$). Generally speaking, for the case of undamped vibration, the motions of the 5 masses are either in phase or completely out of

phase. However, once we introduce viscous damping, there is a phase difference between the responses of the masses.

Mode Shape Matrix

Mathematical terms related to the normal mode of vibration possess dynamic properties associated with the system and may be determined from the simultaneous equations of motion. Another approach is to decouple the equations of motions so that they may be solved independently. This is accomplished using the *mode shape matrix*.

The equations of motion are solved in modal space using the eigensolution (modal properties) of the homogeneous equation of motion for free vibration without viscous damping (Equation 2). Orthogonality properties of the normal modes of vibration are utilized to decouple the equations of motion. A matrix is orthogonal if $P^{-1} = P^{tr}$, where {tr} denotes the transpose, and the determinant of an orthogonal matrix is equal to ± 1. If $[S]$ = symmetric matrix, then $P^{-1}[S]P = D = P^{tr}[S]P$, where D is a *diagonal matrix*. Applying orthogonality to the mass and stiffness matrices we have:

$$[\psi_i]^{tr}[M][\psi_i] = M_{ii} \tag{3a}$$

$$[\psi_i]^{tr}[K][\psi_i] = K_{ii} \tag{3b}$$

where M_{ii} and K_{ii} are the *generalized mass* and *generalized stiffness* matrices, respectively. These are the 2 orthogonality properties of the mass and stiffness matrices for a multi-DOF structure. Using the property of orthogonality, the eigenvectors (mode shapes or modal vectors) are assembled into a *weighted normal mode shape* matrix $[\phi]$ such that:

$$[\phi]^{tr}[M][\phi] = [I] \tag{4a}$$

$$[\phi]^{tr}[K][\phi] = [\Omega^2] \tag{4b}$$

where $[I]$ is the diagonal identity matrix. ϕ is defined as the normal mode shape ψ_i divided by the square root of M_{ii}.

When the normal modes of the system are known, the weighted normal mode matrix or *weighted modal matrix* is used to decouple the equations of motion. We make the coordinate transformation $x = \phi q$ to obtain:

$$[M][\phi]\{d^2q/dt^2\} + [C][\phi]\{dq/dt\} + [K][\phi]\{q\} = \{F\} \tag{5}$$

Next, premultiply by the transpose of ϕ^{tr} to obtain:

$$[\phi^{tr}][M][\phi]\{d^2q/dt^2\} + [\phi^{tr}][C][\phi]\{dq/dt\} + [\phi^{tr}][K][\phi]\{q\} = [\phi^{tr}]\{F\} \tag{6}$$

Because the products $[\phi^{tr}][M][\phi]$, $[\phi^{tr}][C][\phi]$, and $[\phi^{tr}][K][\phi]$ are diagonal matrices due to orthogonality, the new equations in terms of q are uncoupled and can be solved as a system of 1 DOF. The original coordinates x can then be found from the transformation equation $x = \phi q$.

Viscous damping has a large influence on the amplitude of motion in the frequency region near resonance. When the damping term c is large, no oscillations are possible and the structure is referred to as being *overdamped*. Conversely, when c is small or close to zero, oscillatory motion of the structure will continue for many cycles, a condition that is referred to as *underdamped*. Viscous damping can also be expressed in terms of the critical damping c_c (the limiting case between the oscillatory and nonoscillatory motion) using a nondimensional number $\zeta = c/c_c$, called the damping ratio. By defining the modal damping matrix ζ as:

$$[\zeta] = \begin{bmatrix} \zeta_1 & 0 & 0 & 0 & 0 \\ 0 & \zeta_2 & 0 & 0 & 0 \\ 0 & 0 & \zeta_3 & 0 & 0 \\ 0 & 0 & 0 & \zeta_4 & 0 \\ 0 & 0 & 0 & 0 & \zeta_5 \end{bmatrix}$$

where $\zeta_{1...5}$ are the modal damping ratios for each mode shape $i = 1...5$, the 5×5 damping coefficient matrix is computed as:

$$[C] = [M][\phi]2[\zeta][\Omega][\phi]^{tr}[M] \tag{7}$$

Modal damping ratios are analogous to damping ratios used in single DOF systems but are applied independently to each modal or decoupled equation. Hence, modal damping ratios are automatically decoupled.

Applied Forces

Manual therapeutic forces can be can be broadly classified into several categories; however, the most commonly used among clinicians include spinal mobilization, and high-velocity, low-amplitude manipulation. Manipulation can be further categorized as specific contact thrust procedures (delivered by hand), and mechanical-force, manually-assisted (MFMA) procedures (delivered by means of a mechanical device), although many more forms of manipulation application or chiropractic techniques exist.

Mobilization is commonly used during both the assessment and treatment of spinal disorders and involves applying quasi-static (<2.0 Hz) cyclic or oscillatory PA forces (20–100 N peak) to a selected vertebra or several vertebrae.[3,11-13] Both manual and instrument-based (Spinal Physiotherapy Simulator[14]; Spinal Mobilization Apparatus[15]) mobilization assessment and treatments exist. Mobilization forces applied to the lumbar spine typically range from 20 to 100 N peak-to-peak. During mobilization, the spine is forced to vibrate at the same frequency as that of the excitation, and *steady-state* oscillations are produced.

Spinal manipulation involves a specifically vectored high-velocity, low-amplitude thrust that is usually directed in a PA direction.[16] Hence, spinal manipulation differs from mobilization in that the spine is influenced by a suddenly applied nonperiodic excitation. Such excitations are called *transient*, since steady-state oscillations are generally not produced. Manual manipulation applied to the thoraco-lumbar spine are generally associated with higher peak PA forces (typically 250–550 N) but are comparable to mobilization therapy in terms of time to peak force (typically 100-200 ms).[17,18] MFMA procedures utilize a hand-held mechanical instrument to produce a very short duration (typically <5 ms) force-time profile, with peak force amplitudes ranging from 100 to 200 N.[6] Forces that are relatively large in magnitude but act for a very short time (less than the natural period of oscillation) are called *impulsive*. Impulsive forces $\hat{F}$ acting on a mass m will result in a sudden change in velocity proportional to $\hat{F}/m$ but are typically associated with smaller displacements in comparison to longer duration transient forces.

The static displacement response to PA static forces is given by

$$[\bar{x}] = [K]\backslash\{\bar{F}\} \tag{8}$$

where \ denotes matrix division.

The steady-state displacement response to a PA sinusoidal force oscillation, $\tilde{F} = F_0 e^{i\omega t}$ is obtained from the frequency response function: $[H(\omega)] = [K - \omega^2 M + i\omega C]^{-1}$ as

$$[\bar{x}] = \text{real}\,([H(\omega)]/\{\tilde{F}\}) \tag{9}$$

The response to an impulsive force characterized by an initial displacement $[x_0]$ and velocity $[v_0]$ was derived by assuming a solution $x = Ue\lambda^t$ for Equation 1:

$$[\hat{x}] = [\phi]e^{\lambda^t}[\phi]^{-1}[a] + [\phi^*]e^{\lambda^{*t}}[\phi^*]^{-1}[a^*] \tag{10}$$

where $[a] = [\phi][\lambda - \lambda^*]^{-1}[\phi]^{tr}[M]\{[v_0] - [\phi][\lambda^*][\phi]^{tr}[M][x_0]\}$, $\lambda = -[\zeta][\Omega] \pm i[\Omega]\{1 - [\zeta^2]\}^{1/2}$, and * denotes the complex conjugate.

Numerical Simulation and Model Coefficients

Using Matlab (MathWorks, Inc, Natick, Mass), the motion response of the spine was studied in response to a 100 N static load, 100 N sinusoidal oscillation, and 100-N impulsive force applied to the spinous processes each of the vertebral segments.

Although 100 N is representative of forces associated with mobilization and MFMA techniques, this value is somewhat low for specific contact thrust manual manipulation. However, since the displacement response predicted by the model scales either linearly (static forces) or according to k^2 (dynamic forces), the static and dynamic motion response can be readily scaled to higher or lower forces.

The following coefficients were used for the lumbar segment mass matrix $[M]$: $m_1 = m_2 = 0.170$ kg, and $m_3 = m_4 = m_5 = 0.114$ kg. Each mass represented the vertebrae and surrounding tissues and was based upon trunk segment masses coresponding to a 70-kg reference man.[19,20] Modal damping ratios ζ_i for each of the FJSs were assumed to be equal, and the effects of damping were examined by varying the damping ratio $\zeta_{1,\ldots,5}$ between 0.0 and 0.30 (30% of critical), where $\zeta = 0.0$ represents the undamped case and $\zeta = 0.30$ represents heavy damping. The sensitivity of the model to variations in stiffness was also studied. Coefficients for the PA stiffness matrix $[K]$ were chosen based on ranges of values reported in the literature for lumbar intervertebral disks and functional spinal units.[21-23] Accordingly, PA FJS stiffness values k were varied from 25 kN/m to 75 kN/m. Stiffness values k_i for individual lumbar segments were modulated as follows: $k_1 = 1.0k$, $k_2 = 0.8k$, $k_3 = 0.7k$, $k_4 = k_5 = 0.6k$, and $k_6 = 0.9k$. This lumbar stiffness profile was based on studies that have examined human thoracolumbar spine PA stiffness variations to thrusts on the spinous processes.[8,24]

Results

Modes of Vibration

The normal modes of vibration are shown in Figure 2. In the first normal mode, the 5 lumbar segments (masses) move in phase. In the second mode, lumbar segments 1 and 2 are out of phase with respect to segments 3, 4, and 5. Mode 2 has 1 node. In the third mode, lumbar segments 1, 4, and 5 are out of phase with respect to segments 2 and 3. Mode 3 has 2 nodes, both of which are close to lumbar segments 2 and 4. In the fourth mode, segments 1, 3, and 4 are out of phase with respect to segments 2 and 5. Mode 4 has 3 nodes. In the fifth mode, lumbar segments 1, 3, and 5 are out of phase with segments 2 and 4. Mode 5 has 4 nodes.

Influence of the Damping Coefficient

Table 1 summarizes the changes in PA damped natural frequencies associated with varying damping ratio and fixed $k = 50$ kN/m (median value examined in this study). For $\zeta = 0.0$, the model behaves as a harmonic oscillator, and the damped natural frequency equals the undamped natural frequencies. The first undamped natural or resonant frequency of PA vibration ($f_1 = \Omega_1/2\pi$) was 46.1 Hz. The corresponding damped resonant frequency $f_{d1} = \Omega(1 - \zeta^2)/2\pi$ ranged from 44.0 Hz (highly damped) to 46.1 Hz (undamped) over the range of damping ratios examined ($\zeta_i = 0.0–0.30$). Values of $\zeta_i = 0.15$ (15% of critical) were found to produce oscillation time histories that corresponded most closely with experimental observations of the intersegmental motion response of the normal human lumbar spine subjected to impulsive forces.[22] For 15% damp-

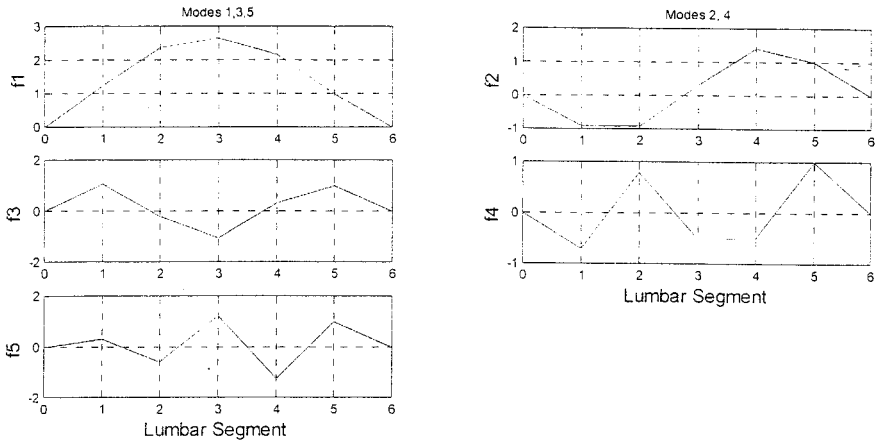

Fig 2. *Mode shapes 1 through 5. The response of each mass is a combination of 5 harmonics that are weighted by the respective modal ratios. Segments 0 and 6 correspond to the thorax and sacrum, respectively, which were assumed to be rigidly fixed.*

Table 1. *Damped natural frequencies (f, Hz) of vibration corresponding to the first five modes of vibration. All values shown are for a PA stiffness k = 50 kN/m*

Damping ratio ζ	f_1	f_2	f_3	f_4	f_5	Gain
0.00	46.08	84.81	121.1	141.3	158.3	1250
0.05	46.03	84.70	121.0	141.1	158.1	7.91
0.10	45.85	84.39	120.5	140.5	157.5	4.01
0.15	45.56	83.85	119.8	139.7	156.5	2.74
0.20	45.15	83.10	118.7	138.5	155.1	2.12
0.25	44.62	82.12	117.3	136.8	153.3	1.75
0.30	43.96	80.91	115.6	134.8	151.0	1.52

ing, the displacement signal gain (displacement at resonance/static displacement) was 2.74 (Table 1). Hereafter, the model results presented will correspond to a damping ratio $\zeta = 0.15$.

Influence of the Stiffness Coefficient

The damped resonant frequency of the lumbar spine decreased to 32.2 Hz when the stiffness coefficient k was decreased to 25 kN/m (Table 2). Increasing k 3-fold to 75 kN/m increased the damped resonant frequency to 55.8 Hz. PA lumbar segment displacements varied in a linear manner over the range of stiffness values examined. For PA forces applied to the L3 spinous process, the L3 static displacement ranged from 2.68 mm ($k = 75$ kN/m) to 8.05 mm ($k = 25$ kN/m) (Table 2). Displacements resulting from oscillatory forces (Equation 9) and impulsive forces (Equation 10) varied approximately 3-fold and 1.7-fold, respectively, over the range of k examined (Table 2). Stiffness values in the range 25 to 50 kN/m produced static PA lumbar segmental displacements that were most consistent with previously published, low-frequency oscillatory experimental responses in human subjects: 4.75 to 6.75 mm,[3] 5.2 to 8.93 mm,[21] and 4.1 to 6.3 mm.[25] PA stiffness values ranging from 35 to 60 kN/m resulted in natural frequencies consistent with experimental results obtained from driving point mechanical impedance studies of the lumbar spine.[26,27] Hereafter, the model results presented will correspond to the median stiffness coefficient $k = 50$ kN/m (and $\zeta = 0.15$).

Static Force PA Motion Response

For the model with the median PA stiffness coefficient ($k = 50$ kN/m) and median damping coefficient ($\zeta = 0.15$), PA displacements of the vertebral bodies at L3 were 1.09 mm, 2.46 mm, 4.03 mm, 2.52 mm, and 1.01 mm for L1, L2, L3, L4, and L5 segments, respectively, for a static force of 100 N. Corresponding intersegmental static displacements were 1.37 mm (L1-L2), 1.56 mm (L2-L3), 1.51 mm (L3-L4), and 1.51 mm (L4-L5).

Steady-State Motion Response

Figure 3 illustrates the oscillatory or steady-state displacement response of selected lumbar vertebrae subjected to a 100-N force on L3. Segmental and intersegmental steady-state displacement responses for frequencies corresponding to PA spine mobilization and manual manipulation ($\approx$2 Hz), segmental (L3), and intersegmental (L3-L4)

Table 2. *Influence of stiffness on damped natural frequency (f_{d1}), peak L3 PA static force displacement, peak L3 PA oscillatory force displacement and peak-peak L3 PA impulsive force displacement*

Stiffness k (kN/m)	Damped Natural Frequency, f_{d1} (Hz)	L3 Static Force Displacement $\bar{x}$ (mm)	L3 Oscillatory Force Displacement @ f_{d1}, $\tilde{x}$ (mm)	L3 Impulsive Force Displacement $\hat{x}$ (mm)
25	32.2	8.05	22.1	2.45
30	35.3	6.71	18.4	2.24
35	38.1	5.75	15.8	2.07
40	40.8	5.03	13.8	1.94
45	43.2	4.47	12.3	1.83
50	45.6	4.03	11.0	1.73
55	48.3	3.66	10.0	1.65
60	49.9	3.36	9.20	1.58
65	52.0	3.10	8.49	1.52
70	53.9	2.88	7.88	1.46
75	55.8	2.68	7.36	1.41

All values shown are for thrusts on L3 spinous process and damping ratio $\zeta = 0.15$. Boxed regions show ranges of values for in vivo experiments.

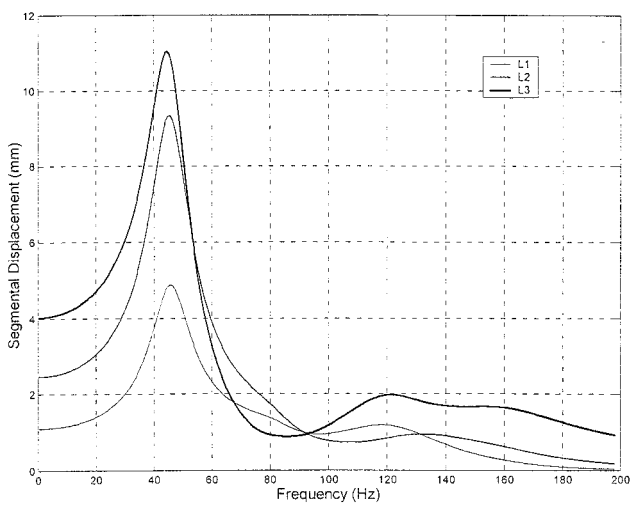

Fig 3. *Effect of PA oscillatory frequency on the displacement response of the L1, L2, and L3 vertebrae. A 100-N oscillatory force was applied to the L3 spinous process. Model results shown are for median values of k (50 kN/m) and ζ (0.15).*

displacements were nearly identical to the static displacement response. At resonance, peak segmental PA displacements increased 2.74-fold to 4.88 mm (L1 @ 45.7 Hz), 9.34 mm (L2 @ 45.8 Hz), 11.0 mm (L3 @ 44.9 Hz), 8.78 mm (L4 @ 45.1 Hz), and 3.98 mm (L5 @ 45.3 Hz). Peak-to-peak intersegmental steady-state displacements were 4.47 mm (L1-L2), 1.69 mm (L2-L3), 2.26 mm (L3-L4), and 4.80 (L4-L5) at the first natural frequency. The oscillatory displacement response was markedly attenuated for oscillatory forces above approximately 80 Hz.

Impulsive Force Motion Response

PA MFMA adjustments produce a damped, sinusoidal-like force-time history with a duration of ≈5 ms (impulsive force), which was approximated as: $F = 466e^{-1000t}\sin(200\pi t)$. We used the impulse-momentum principle to estimate the initial velocity

$$V_0 = \frac{1}{m}\int F dt = 1.8414 \text{ m/s}$$

for an exponentially damped MFMA oscillation. Using Equation 10 with $x_0 = 0$, a 5-ms impulsive force at L3 produced segmental (Fig 4, *A*) and intersegmental (Fig 4, *B*) displacement oscillations over a time period of approximately 100 ms. PA impulsive forces produced appreciable segmental and intersegmental displacements in adjacent vertebrae (Fig 5). Segmental and intersegmental displacements ranged from 0.67 mm (L5) to 1.55 mm (L3), and 0.79 mm (L1-L2) to 1.13 mm (L2-L3), respectively, for impulsive forces at L3 (Figs 5, *A* and *B*). Intersegmental motions were greatest for forces applied at L1 (1.61 mm at L1-L2) and L5 (1.44 mm at L4-L5).

Discussion

The purpose of this investigation was to develop an analytical model to predict the static and dynamic lumbar spine motion response of the human spine subjected to PA forces consistent with chiropractic manipulative procedures. Original published data from quasi-static or oscillatory force loads associated with mobilization[3,21,25] and those applied in high-velocity, low-amplitude (HVLA) spinal manipulation[17] and mechanical-force, manually-assisted spinal adjustments[22] were used to validate the model predictions. A modal damping ratio of 0.15 and stiffness coefficients ranging from 25 to 60 kN/m produced damped natural frequencies and static force PA displacements consistent with these studies.

In this study we have assumed that the lumbar spine could be modeled as an assemblage of homogeneous rigid

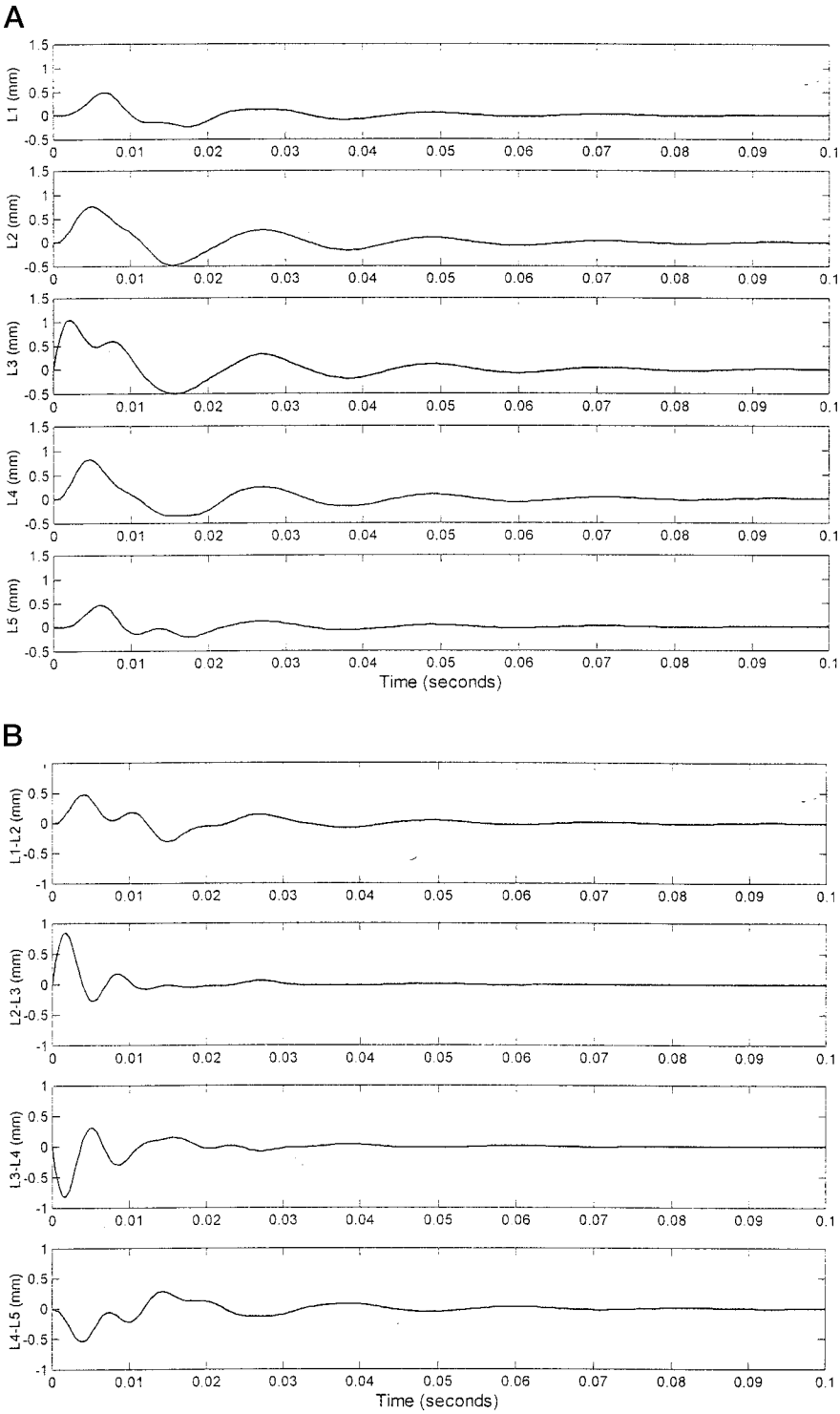

Fig 4. **A**, *Lumbar segmental PA displacement-time history responses to 100-N impulsive force at L3.* **B**, *Lumbar intersegmental PA displacement-time history responses to 100-N impulsive force at L3. Model results shown are for median values of k (50 kN/m) and ζ (0.15).*

masses (vertebrae and surrounding tissues) connected by flexible linkages consisting of simple spring and damper elements. One advantage of the rigid body system approach (also called *lumped parameter system approach*) is that Newton's Second Law can be applied to all vertebral masses to obtain a set of differential equations that completely describes the dynamics of the system, including inertial, dissipative (viscous), and restorative force re-

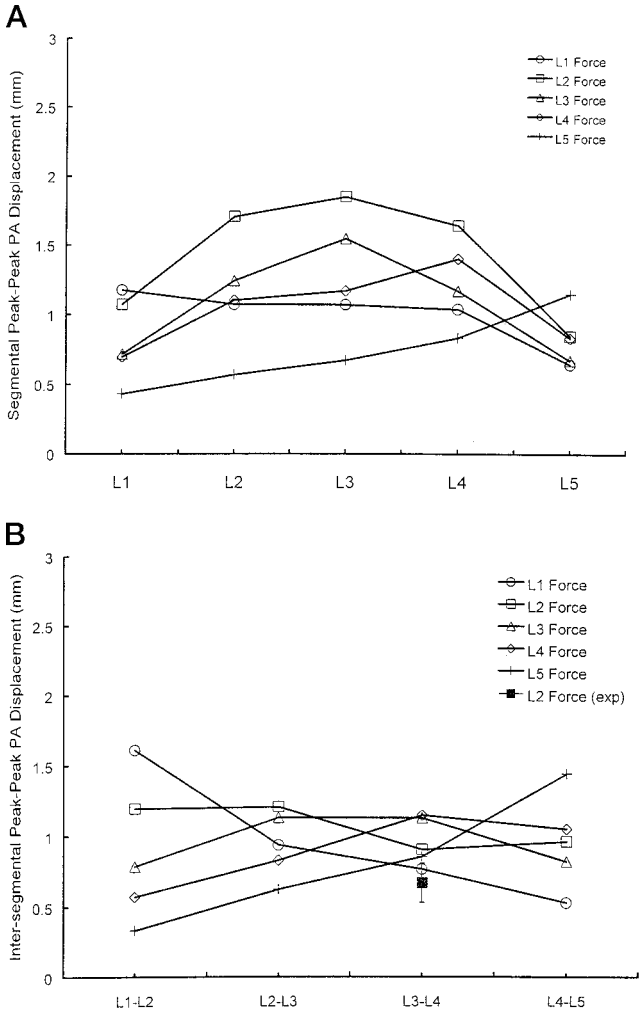

Fig 5. A, *Lumbar segmental peak-to-peak PA displacement responses to 100-N impulsive forces applied to the L1, L2, L3, L4, and L5 spinous processes.* **B**, *Lumbar intersegmental peak-to-peak PA displacement responses to 100-N impulsive forces applied to the L1, L2, L3, L4, and L5 spinous processes, together with experimental data. Model results shown are for median values of k (50 kN/m) and ζ (0.15).*

sponses. As shown here, the differential equations can be solved analytically in matrix form to obtain structural responses to specified external forces and boundary conditions. Alternatively, more computationally and computer memory-intensive methods such as the finite element method can be used to model the dynamics of posteroanterior spine motion as a more complex, nonhomogeneous assemblage of many smaller elements,such as plates and beams. In this manner, the various soft tissue and hard tissue components of the spine (intervertebral disks, ligaments, and facet joints) can be modeled discretely by defining material properties for each individual structure. However, the lumped parameter modeling approach used in this study greatly simplifies the analysis without significant loss of accuracy, as evidenced by the fact that the salient features of the PA static and dynamic motion response of the human spine were well reproduced.

From the point of view of application of the model to characterize manipulative forces, a limitation of the current model is the fact that only PA motions in response to PA-directed thrusts can be determined. Clinical chiropractic therapies applied to the spine generally involve the application of thrusts that are directed along a specific line of drive and are not necessarily aligned with the transverse axis of the vertebrae. Therefore, for the model to be more realistic, additional degrees of freedom should be added, such that it is possible to predict transverse displacements, axial displacements, and rotational responses to SMT thrusts applied along complex load vectors. The present model is also based on the assumption that the vertebrae can be considered rigid structures, when in fact they are elastic, if not inelastic, structures exhibiting nonlinear load-displacement behavior. Moreover, the more flexible intervertebral joints (intervertebral disks and facet joints) show a highly nonlinear load-displacement behavior, particularly for low forces and forces near the elastic limit where the stiffness is considerably lower compared to the elastic region. Hence, the model predictions are most applicable to forces in the elastic loading zone and will tend to underestimate the static and dynamic motion response for very low-loading or very high-loading situations. The results presented also only pertain to forces applied to a single vertebra and localized to spinous processes. However, the model is easily generalizable to situations in which the applied manipulative force is distributed over 2 or more vertebrae. This model was also limited to predicting the vertebral and intervertebral motion responses along a single axis (PA) and did not consider the influence of the thorax and pelvis. Since the thorax and pelvis are relatively large masses and stiff structures compared to the lumbar vertebrae, the fact that we have not incorporated them into the current model would not be expected to alter the PA motion response appreciably. However, these structures become important when considering the dynamic axial and/or rotational mechanical properties of the lumbar spine, the former characterized by an axial natural frequency of about 5 Hz, which is substantially lower than the 46 Hz PA damped natural frequency predicted by the median damping ratio model.

Clinical and research instrumentation has been developed to assess the in vivo PA response of the spine, the spinal stiffness, or the load/displacement response.[3,6,13,21,25,28-30] Overall, the model static and low-frequency oscillatory segmental displacement predictions showed reasonably good agreement with displacement data reported in these studies. The median model PA lumbar stiffness coefficient examined in this study, however, is appreciably higher than the typical 10- to 20-kN/m lumbar segmental stiffness values that are obtained by low-frequency mobilization experiments in human subjects.[12,13,21,25] Consequently, the me-

dian model tended to underestimate the in vivo PA segmental displacement response of the spine.

Some authors[31] have recently have reported PA stiffness coefficients for the lumbar spine (2.6-3.2 kN/m) that are less than stiffness values reported for skin (6 kN/m).[32] Our model PA segmental displacement predictions are most consistent with skin compliance corrected experimental results published by Lee and Svensson.[3] These authors point out that there are significant load-deformation nonlinearities associated with skin deformation during mobilization experiments, particularly for experiments performed at relatively low-force ranges (<100 N). Latimer et al[12] found that the PA stiffness of the spine decreased over 50% when the data were examined over very low force ranges (30-80 N) in comparison to higher force ranges (137-200 N). The results presented in the current model are based on the assumption that the PA load-deformation response of the spine is linear, and hence our results are not applicable to low-force or quasi-static loading situations.

Discrepancies between model predictions and mobilization experiments may also reflect the fact that we assumed that the contribution of the thorax and pelvis are negligible. Using a sagittal plane finite element model of the spine, ribcage, and pelvis, Lee et al[8] noted that pelvic rotations were on the order of 1.8° to 2.1° per 100 N of applied PA static force at L3. Such rotations would therefore be expected to produce small fluctuations in the force-deformation behavior of the lumbar vertebrae. In addition, the thorax may contribute significantly to the deformation behavior of the lumbar spine subjected to PA forces. Experimental studies have shown that the stiffness of the thorax is about 200 kN/m.[21] Although this is approximately 3- to 8-fold stiffer than the range of PA lumbar stiffness examined in the current study, rigid body modeling of the thorax may further reduce discrepancies of model predictions and in vivo experiments. Additional research is needed to study the influence of stiffness characteristics of the pelvis and thorax, as well as boundary conditions reflecting thorax and pelvis constraints for a prone-lying subject, on the PA rigid body dynamics of the lumbar spine.

The model-predicted PA natural frequency of the lumbar spine is consistent with recent dynamic transfer function experiments performed using a mechanical impedance assessment procedure.[6,24,27] These studies indicate that for frequencies greater than 10 Hz, the spine is most mobile for forces applied at frequencies ranging from 38 to 50 Hz. A similar frequency range was reproduced for a damping ratio of 0.15 and PA stiffness coefficients ranging from 35 to 60 kN/m. Our model, however, tended to overestimate PA intersegmental displacements associated with impulsive force types of spinal manipulation (MFMA). Stiffness coefficients greater than 50 kN/m are required to correctly model the L3-L4 intersegmental motion response of the human spine reported by Nathan and Keller.[22] These authors used an intervertebral motion device (IMD) attached to the L3-L4 spinous processes to quantify intersegmental motion responses to PA MFMA forces (72 N) on the adjacent L2 lumbar spinous process. In the one normal subject examined, the average L2 PA stiffness was 62 kN/m, and the average intersegmental L3-L4 displacements was 0.48 mm (0.67 mm after correcting for the 28-N force difference). An increase in the model PA stiffness coefficient to 92 kN/m would be required to precisely match these intersegmental displacement data. Additional experimental validation of the dynamic PA oscillatory and PA impulsive force response of lumbar spine is needed to more precisely establish model coefficients and to confirm the general validity of the model.

Noteworthy was our finding that, while segmental displacements were over 3-fold greater for manual and mobilization therapies in comparison to MFMA therapy, differences in intersegmental displacements were much less remarkable for these interventions. From a clinical standpoint, intersegmental motions are considered important therapeutically. Rapid distraction of the functional spinal unit as applied in spinal manipulation is hypothesized to release entrapped synovial folds, relax hypertonic muscles, disrupt articular or periarticular adhesions, and unbuckle functional spinal units that have undergone disproportionate displacements.[33] While evidence has yet to substantiate these concepts, concomitant neuromuscular reflex responses associated with spinal manipulation are promising,[34-36] as afferent stimulation is been attributed to nociceptive inhibition.[37] Such responses are thought to originate from stimulation of mechanosensitive afferents in the discoligamentous and muscular soft tissues of the spine on distraction[38] or other mechanical stimulation.[39] It remains to be seen whether intersegmental motions contribute more to afferent stimulation than segmental motions occurring during range of motion efforts.[40]

Reflex effects associated with spinal manipulation have not been found to be related to the magnitude of force application, but rather the rate at which the force is applied.[41] Of further interest is the frequency at which the thrust is applied during spinal manipulation.[3] In the current study, for loading frequencies corresponding to the natural frequency, there was an appreciable increase in segmental motion compared to static loading. This gain or amplification effect has been observed during axial vibration loading of the spine, for which chronic vibrations at or near resonance are generally regarded as detrimental to the spine.[42] However, from the standpoint of spinal manipulation, motion amplification may be of clinical importance, since this behavior suggests that segmental and intersegmental vertebral motions and oscillations can be produced by lower forces during manipulative procedures if the forces are delivered at or near the natural frequency. The results of the present study indicates that PA forces delivered at or near the natural frequency of the spine will produce a greater segmental and intersegmental motion response in compari-

son to PA forces delivered at other frequencies. Such knowledge and further research may serve to assist clinicians in determining appropriate force-time profiles to apply to patients in different clinical circumstances and may ultimately serve to allow better understanding of how the spine reacts to applied forces during both clinical assessments and therapeutic applications.

Conclusion

In summary, the simple analytical model presented in this study can be used to predict the static, cyclic, and impulsive force PA displacement response of the lumbar spine. The model provides data on segmental and intersegmental motion patterns that are otherwise difficult to obtain experimentally. Such information serves to not only to assist in understanding the biomechanics of therapeutic PA forces applied to the lumbar spine but may ultimately be used to validate chiropractic assessments, characterize spinal motions in response to applied forces by clinicians, and minimize risk to patients receiving spinal manipulative therapy.

Acknowledgments

We acknowledge the National Institute of Chiropractic Research, NASA Experimental Program to Stimulate Competitive Research, and the Foundation for the Advancement of Chiropractic Education. We thank Madhavi Nathan and Jean-Guy Beliveau, PhD, for numerous technical contributions.

References

1. Haldeman S, Chapman-Smith D, Petersen DM. Guidelines for chiropractic quality assurance and practice parameters. Gaithersburg (M): Aspen; 1993.
2. Henderson D, Chapman-Smith D, Mior S, Vernon H. Clinical guidelines for chiropractic practice in Canada. Toronto: Canadian Chiropractic Association; 1993.
3. Lee M, Svensson NL. Effect of loading frequency on response of the spine to lumbar posteroanterior forces. J Manipulative Physiol Ther 1993;16:439-46.
4. Herzog W. Clinical biomechanics of spinal manipulation. Philadelphia: Churchill Livingstone; 2000.
5. Osterbauer PJ, Fuhr AW, Hildebrandt RW. Mechanical force, manually assisted short lever chiropractic adjustment. J Manipulative Physiol Ther 1992;15:309-17.
6. Keller TS, Colloca CJ, Fuhr AW. Validation of the force and frequency characteristics of the activator adjusting instrument: effectiveness as a mechanical impedance measurement tool. J Manipulative Physiol Ther 1999;22:75-86.
7. Rostedt M, Ekstrom L, Broman H, Hansson T. Axial stiffness of human lumbar motion segments, force dependence. J Biomech 1998;31:503-9.
8. Lee M, Kelly DW, Steven GP. A model of spine, ribcage and pelvic responses to a specific lumbar manipulative force in relaxed subjects. J Biomech 1995;28:1403-8.
9. Lee RYW, Evans JH. Towards a better understanding of spinal posteroanterior mobilisation. Physiotherapy 1994;80: 68-73.
10. Solinger AB. Theory of small vertebral motions: an analytical model compared to data. Clin Biomech 2000;15:87-94.
11. Lee M, Steven GP, Crosbie J, Higgs RJ. Variations in posteroanterior stiffness in the thoracolumbar spine: preliminary observations and proposed mechanisms. Phys Ther 1998;78: 1277-87.
12. Latimer J, Lee M, Adams RD. The effects of high and low loading forces on measured values of lumbar stiffness. J Manipulative Physiol Ther 1998;21:157-63.
13. Viner A, Lee M, Adams R. Posteroanterior stiffness in the lumbosacral spine. The correlation between adjacent vertebral levels. Spine 1997;22:2724-9.
14. Lee M, Svensson NL. Measurement of stiffness during simulated spinal physiotherapy. Clin Phys Physiol Meas 1990;11: 201-7.
15. Allison GT, Edmondston SJ, Roe CP, Reid SE, Toy DA, Lundgren HE. Influence of load orientation on the posteroanterior stiffness of the lumbar spine. J Manipulative Physiol Ther 1998;21:534-8.
16. Triano J. The mechanics of spinal manipulation. In: Herzog W, editor. Clinical biomechanics of spinal manipulation. Philadelphia: Churchill Livingstone; 2000. p. 92-190.
17. Gal J, Herzog W, Kawchuk G, Conway PJ, Zhang YT. Movements of vertebrae during manipulative thrusts to unembalmed human cadavers [see comments]. J Manipulative Physiol Ther 1997;20:30–40.
18. Herzog W, Conway PJ, Kawchuk GN, Zhang Y, Hasler EM. Forces exerted during spinal manipulative therapy. Spine 1993;18:1206-12.
19. Ruff S. Brief acceleration: less than one second. Ger Aviat Med World War II 1950;1:584-97.
20. Keller TS, Nathan M. Height change caused by creep in intervertebral discs: a sagittal plane model. J Spinal Disord 1999;12:313-24.
21. Lee M, Liversidge K. Posteroanterior stiffness at three locations in the lumbar spine. J Manipulative Physiol Ther 1994; 17:511-6.
22. Nathan M, Keller TS. Measurement and analysis of the in vivo posteroanterior impulse response of the human thoracolumbar spine: a feasibility study. J Manipulative Physiol Ther 1994; 17:431-41.
23. White A, Panjabi MM. Clinical Biomechanics of the Spine. 2nd ed. Philadelphia: Lippincott-Raven; 1990.
24. Keller TS, Colloca CJ, Fuhr AW. In vivo transient vibration analysis of the normal human thoracolumbar spine. J Manipulative Physiol Ther 2000;23:521-30.
25. Latimer J, Goodsel MM, Lee M, Maher CG, Wilkinson BN, Moran CC. Evaluation of a new device for measuring responses to posteroanterior forces in a patient population. Part 1: reliability testing. Phys Ther 1996;76:158-65.
26. Colloca CJ, Keller TS, Gunzburg R, Van de Putte K, Fuhr AW. Neurophysiological response to intraoperative lumbosacral spinal manipulation. J Manipulative Physiol Ther 2000; 23:447-57.
27. Colloca CJ, Keller TS, Seltzer DE, Fuhr AW. Mechanical impedance of the human lower thoracic and lumbar spine exposed to in vivo posterior-anterior manipulative thrusts. Proceedings of the 12th Conference of the European Society of Biomechanics; Dublin, Ireland, 2000 August 27-30. European Society of Biomechanics; 2000. p. 171.
28. Kawchuk G, Herzog W. A new technique of tissue stiffness (compliance) assessment: its reliability, accuracy and comparison with an existing method. J Manipulative Physiol Ther 1996;19:13-8.
29. Kawchuk GN, Fauvel OR, Dmowski J. Ultrasonic quantifica-

tion of osseous displacements resulting from skin surface indentation loading of bovine para-spinal tissue. Clin Biomech 2000;15:228-33.
30. Kawchuk GN, Fauvel OR, Dmowski J. Ultrasonic indentation: a procedure for the noninvasive quantification of force-displacement properties of the lumbar spine. J Manipulative Physiol Ther 2001;24:149-56.
31. Brodeur RRDL. Stiffness of the thoracolumbar spine for subjects with and without low back pain. J Neuromusculoskeletal Syst 1999;7:127-33.
32. Bader DL, Bowker P. Mechanical characteristics of skin and underlying tissues in vivo. Biomaterials 1983;4:305-8.
33. Shekelle PG. Spinal manipulation. Spine 1994;19:858-61.
34. Colloca CJ, Keller TS. Electromyographic reflex response to mechanical force, manually-assisted spinal manipulative therapy. Spine 2001;26:1117-24.
35. Herzog W, Scheele D, Conway PJ. Electromyographic responses of back and limb muscles associated with spinal manipulative therapy. Spine 1999;24:146-52.
36. Keller TS, Colloca CJ. Mechanical force spinal manipulation increases trunk muscle strength assessed by electromyography: a comparative clinical trial. J Manipulative Physiol Ther 2000;23:585-95.
37. Bonica JJ. The management of pain. 2nd ed. Philadelphia: Lea & Febiger; 1990.
38. Pickar JG, McLain RF. Responses of mechanosensitive afferents to manipulation of the lumbar facet in the cat. Spine 1995;20:2379-85.
39. Cavanaugh JM, Ozaktay AC, Yamashita HT, King AI. Lumbar facet pain: biomechanics, neuroanatomy and neurophysiology. J Biomech 1996;29:1117-29.
40. Bolton PS. Reflex effects of vertebral subluxations: the peripheral nervous system. An update. J Manipulative Physiol Ther 2000;23:101-3.
41. Herzog W. On sounds and reflexes. J Manipulative Physiol Ther 1996;19:216-8.
42. Pope MH, Magnusson M, Hansson T. The upper extremity attenuates intermediate frequency vibrations. J Biomech 1997;30:103-8.

Access to ***Journal of Manipulative and Physiological Therapeutics Online***
is available for print subscribers!

Full-text access to ***Journal of Manipulative and Physiological Therapeutics Online*** is available for all print subscribers. To activate your individual online subscription, please visit ***Journal of Manipulative and Physiological Therapeutics Online***, point your browser to ***http://www.mosby.com/jmpt***, follow the prompts to **activate your online access**, and follow the instructions. To activate your account, you will need your subscriber account number, which you can find on your mailing label (*note:* the number of digits in your subscriber account number varies from 6 to 10). See the example below in which the subscriber account number has been circled:

Sample mailing label

This is your subscription account number

**********3-DIGIT 001
SJ P1
AUG00 J076 C: 1 1234567-89 U 05/00 Q:1
J. H. DOE, MD
531 MAIN ST
CENTER CITY, NY 10001-001

Personal subscriptions to ***Journal of Manipulative and Physiological Therapeutics Online*** are for individual use only and may not be transferred. Use of ***Journal of Manipulative and Physiological Therapeutics Online*** is subject to agreement to the terms and conditions as indicated online.